Title

Emotion Downregulation Targets Interoceptive Brain Regions While Emotion Upregulation Targets Other Affective Brain Regions.

Journal

Journal of Neuroscience, 42(14)

Authors

Min, Jungwon

Nashiro, Kaoru

Yoo, Hyun

et al.

Publication Date

2022-04-06

DOI

10.1523/JNEUROSCI.1865-21.2022

Peer reviewed

Behavioral/Cognitive

Emotion Downregulation Targets Interoceptive Brain Regions While Emotion Upregulation Targets Other Affective Brain Regions

Jungwon Min,[1] Kaoru Nashiro,[1] Hyun Joo Yoo,[1] Christine Cho,[1] Padideh Nasseri,[1] Shelby L. Bachman,[1] Shai Porat,[1] Julian F. Thayer,[2] Catie Chang,[3] Tae-Ho Lee,[4] and Mara Mather[1]

[1]University of Southern California, Los Angeles, California 90089, [2]University of California, Irvine, California 92697, [3]Vanderbilt University, Nashville, Tennessee 37235, and [4]Virginia Tech, Blacksburg, Virginia 24061

Researchers generally agree that when upregulating and downregulating emotion, control regions in the prefrontal cortex turn up or down activity in affect-generating brain areas. However, the "affective dial hypothesis" that turning up and down emotions produces opposite effects in the same affect-generating regions is untested. We tested this hypothesis by examining the overlap between the regions activated during upregulation and those deactivated during downregulation in 54 male and 51 female humans. We found that upregulation and downregulation both recruit regulatory regions, such as the inferior frontal gyrus and dorsal anterior cingulate gyrus, but act on distinct affect-generating regions. Upregulation increased activity in regions associated with emotional experience, such as the amygdala, anterior insula, striatum, and anterior cingulate gyrus as well as in regions associated with sympathetic vascular activity, such as periventricular white matter, while downregulation decreased activity in regions receiving interoceptive input, such as the posterior insula and postcentral gyrus. Nevertheless, participants' subjective sense of emotional intensity was associated with activity in overlapping brain regions (dorsal anterior cingulate, insula, thalamus, and frontal pole) across upregulation and downregulation. These findings indicate that upregulation and downregulation rely on overlapping brain regions to control and assess emotions but target different affect-generating brain regions.

Key words: **arousal; downregulation; emotion; fMRI; interoception; upregulation**

Significance Statement

Many contexts require modulating one's own emotions. Identifying the brain areas implementing these regulatory processes should advance understanding emotional disorders and designing potential interventions. The emotion regulation field has an implicit assumption we call the affective dial hypothesis: both emotion upregulation and downregulation modulate the same emotion-generating brain areas. Countering the hypothesis, our findings indicate that up- and down-modulating emotions target different brain areas. Thus, the mechanisms underlying emotion regulation might differ more than previously appreciated for upregulation versus downregulation. In addition to their theoretical importance, these findings are critical for researchers attempting to target activity in particular brain regions during an emotion regulation intervention.

Introduction

As humans, we can strategically modulate our own emotions. Often, this involves diminishing negative emotions and intensifying positive emotions. But there are also situations when one would want to increase the intensity of negative emotions (e.g., when wanting to feel empathy for a friend's grief) or decrease the intensity of positive emotions (e.g., when trying not to laugh at a child's embarrassing mistake). Thus, both diminishing and intensifying processes operate across positive and negative emotions (Gross, 2015).

Prior neuroimaging research indicates that diminishing and intensifying emotion rely on a shared set of affect-controlling regions that modulate activity in affect-generating regions

Received Sep. 14, 2021; revised Jan. 6, 2022; accepted Jan. 31, 2022.

Author contributions: J.M., K.N., H.J.Y., J.F.T., C. Chang, and M.M. designed research; J.M., K.N., H.J.Y., C. Cho, P.N., S.L.B., and S.P. performed research; J.M., K.N., and M.M. analyzed data; J.M. wrote the first draft of the paper; J.M., K.N., H.J.Y., C. Cho, P.N., S.L.B., S.P., J.F.T., C. Chang, T.L., and M.M. edited the paper; J.M. and M.M. wrote the paper; T.L. contributed unpublished reagents/analytic tools.

This work was supported by National Institutes of Health R01AG057184 to M.M. We thank our research assistants for help with data collection: Linette Bagtas, Akanksha Jain, Divya Suri, Sophia Ling, Michelle Wong, Yong Zhang, Vardui Grigoryan, and Gabriel Shih.

The authors declare no competing financial interests.

Correspondence should be addressed to Mara Mather at mara.mather@usc.edu.

https://doi.org/10.1523/JNEUROSCI.1865-21.2022

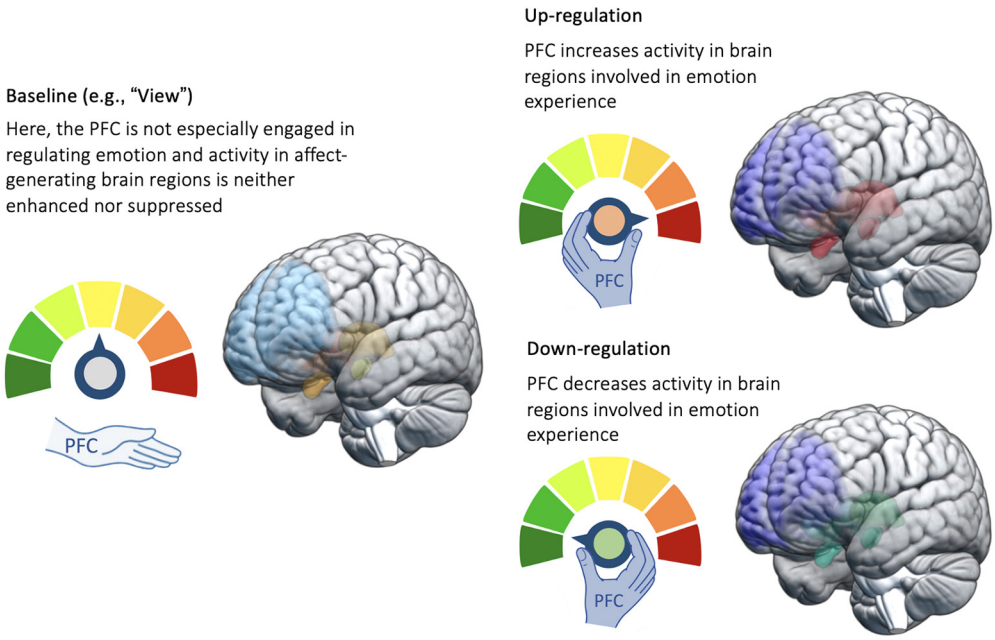

Figure 1. Schematic view of the affective dial hypothesis. The control system (hand) dials down activity in affect-generating brain regions during emotion downregulation and dials up activity in these same target regions during upregulation. Simply viewing emotional images activates affect-generating brain regions without the action of the control system.

(Ochsner et al., 2012; Buhle et al., 2014). This set of affect-control regions includes the ventrolateral prefrontal cortex (PFC), dorsomedial PFC, and dorsolateral PFC (Ochsner et al., 2012; Kohn et al., 2014; Morawetz et al., 2017b). On the other hand, the amygdala, insula, and striatum have been identified as affect-generating regions (Phelps, 2006; Craig, 2009; Grosse Rueschkamp et al., 2019), which can be up- or down-modulated by the control system (Ochsner et al., 2012; Braunstein et al., 2017).

Despite its wide acceptance, the idea of the control system's dialing up or down activity in affect-generating regions relies on an untested assumption: upregulating (i.e., trying to intensify one's emotions) will increase activity in the same affect-generating brain regions that downregulating (i.e., trying to diminish one's emotions) will decrease activity in. We call this implicit assumption of the emotion regulation field the "affective dial hypothesis" (Fig. 1). Indeed, we initially assumed we would see affective-dial-like effects; however, our findings made us realize we needed to rethink this assumption.

There are at least 11 prior studies with young adults that included both upregulation and downregulation trials as well as a nonregulation control and so could provide evidence to support the affective dial hypothesis (Ochsner et al., 2004; Eippert et al., 2007; Kim and Hamann, 2007; Domes et al., 2010; Leiberg et al., 2012; Morawetz et al., 2016a,b, 2017a; Li et al., 2018; Steinfurth et al., 2018; Sokołowski et al., 2021), most of which were reported in a recent meta-analysis (Morawetz et al., 2017b). These studies typically showed increased activity in the ventrolateral PFC, dorsolateral PFC, supplementary motor area, and anterior cingulate gyrus (ACC) during both intensifying and diminishing emotion. Furthermore, five of these studies included an explicit test of which regions were involved in regulation in both conditions by examining where overlap occurred between the upregulation > baseline and downregulation > baseline contrasts (Eippert et al., 2007; Leiberg et al., 2012; Morawetz et al., 2016a, 2017a; Li et al., 2018). All five of these studies showed some overlap between these two contrasts. Thus, these overlapping regions are involved in emotional control regardless of whether people are trying to upregulate or downregulate their emotions. However, the affective dial idea that the same affect-generating regions are targeted by upregulation and downregulation currently lacks support. None of those 11 studies reported an explicit test of the overlap between upregulate > baseline and baseline > downregulate contrasts.

The current study provides strong power ($N = 105$) to test the affective dial hypothesis. We included both upregulation and downregulation trials within the same session and contrasted them with viewing trials, allowing us to examine how much the targets of upregulation and downregulation overlap. We then used brain maps from a prior meta-analytic study which investigated the shared and unique brain regions activated by emotion, interoception, and social cognition (Adolfi et al., 2017) to characterize the nature of the regions modulated by upregulation and downregulation. To follow-up on our surprising findings showing mostly different targets of downregulation and upregulation, we conducted exploratory analyses examining whether participants' subjective sense of emotional intensity correlated with activity in the same or different brain regions during downregulation versus upregulation attempts.

Materials and Methods

Participants. The emotion regulation task was conducted as part of a 5-week heart rate variability biofeedback intervention study in which participants were randomly assigned to daily sessions of biofeedback to either increase or decrease their heart rate oscillatory activity (www.ClinicalTrials.gov identifier: NCT03458910). The emotion regulation task was conducted both before and after the interventions, but for this paper we just used the baseline data from young adults before any intervention was conducted. The N was determined to provide power to detect medium effect size differences between the two intervention groups. For the baseline data, the N provides 80% power to detect small-to-medium within-subject effects (i.e., $d = 0.28$) (Faul et al., 2007). Participants were recruited via University of Southern California's subject pool, University of Southern California's online bulletin board, Facebook, and flyers, and screened out for medical or psychiatric illnesses. However, people taking antidepressant or antianxiety medication were excluded only if they anticipated a change in treatment during the

Figure 2. Emotion regulation trial design.

intervention. Participants received $15 per hour for the baseline laboratory visit, which lasted around 2.5 h and included cognitive and emotional tasks and magnetic resonance imaging (MRI) scans. The MRI scans included resting-state blood-oxygenation-level-dependent (BOLD), resting-state arterial spin labeling, emotion regulation task, and structural scans, in that order. Ninety-five participants provided MRI scans for the emotion regulation task for both pre- and post-intervention sessions. As the present analyses focused on the pre-intervention session, we included 19 participants who dropped out after the first emotion regulation task. We excluded 6 participants because they did not respond to ratings for more than half of the trials. We also excluded 3 participants because of failed multiecho independent component analysis (ME-ICA) preprocessing. This yielded 105 participants who ranged in age from 18 to 31 years (M_{age} = 22.8, SD_{age} = 2.69) and consisted of 54 males and 51 females.

Task. We based our study design on a previously validated emotion regulation task (Kim and Hamann, 2007), which has upregulation and downregulation trials for positive and negative emotions. We used an event-related design. The 10-min emotion regulation task had 42 trials, each of which consisted of a sequence involving a 1-s instruction, a 6-s regulation, and a 4-s rating period (Fig. 2). During the 6-s regulation period, participants were asked to regulate emotion induced by the images according to the presented instruction. The instructions were "intensify," "diminish," or "view," and the presented images were positive, negative, or neutral. Pairing of the instructions and images yielded seven conditions: diminish-negative, diminish-positive, intensify-negative, intensify-positive, view-negative, view-positive, and view-neutral. After regulation, participants were asked to rate their strength of feeling with a scale from 1 (weak) to 4 (strong). Three trials from each condition were nested in a mini-block where the trials were separated by a fixation cross with a jittered interval that ranged from 0 to 4 s. The jittered intervals summed up to 4 s to keep the mini-block length the same, and the mini-blocks were spaced apart by a 5-s-long fixation cross. A total of 14 mini-blocks were arranged in a pseudorandom manner such that no blocks with the same instruction or image valence were shown consecutively. Six sets of images were selected from the International Affective Picture System. Each set consisted of 18 negative ($M_{valence}$ = 2.8, $M_{arousal}$ = 5.4), 18 positive ($M_{valence}$ = 7.2, $M_{arousal}$ = 5.4), and 6 neutral images ($M_{valence}$ = 5.0, $M_{arousal}$ = 2.8), with their average valence and arousal scores the same across the six sets. During the task, each participant was presented with the 42 images in one of the six sets in a randomized order.

Procedure. Participants had a practice session where they came up with their own reappraisal strategies to amplify, moderate, or passively experience the image-induced emotion according to the "intensify," "diminish," or "view" instruction. If they had difficulty devising their own method, they were presented with examples, such as reinterpreting the situations or changing the distance between themselves and the scene. We also advised them to adjust their emotional intensity in the moment rather than generating an emotion opposite to the one that they were experiencing. For example, they were not supposed to replace a negative feeling with a positive one to diminish negative emotion. After the scan, participants were asked to report what regulation strategies they used and how successful they were in regulating emotions. For the four emotion-regulating conditions (e.g., diminish positive), 96%-99% of participants used cognitive reappraisal and 92%-98% of participants reported medium to high levels (3-5) of confidence in their emotion regulation success (1: not successful at all; 3: moderately successful; 5: very successful). The reported strategies mainly fell into two categories: reinterpretation and distancing. For example, the participants tended to rationalize the situation or separate themselves from the scene for downregulation and exaggerate the consequences or personalize the scene for upregulation.

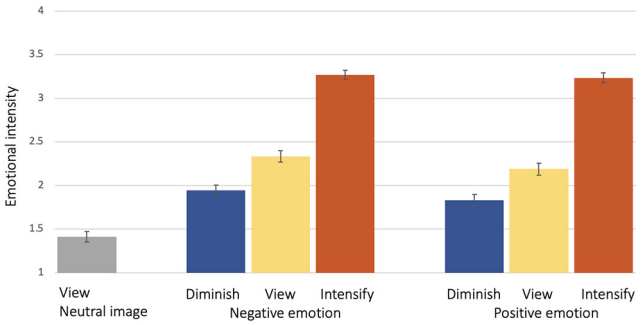

Figure 3. Ratings of emotional intensity. Error bars indicate SE of each condition.

Table 1. Emotional intensity ratings across regulation and valence

	Negative			Positive		
	Mean	SE	95% CI	Mean	SE	95% CI
Diminish	1.95	0.06	[1.82, 2.07]	1.83	0.07	[1.70, 1.96]
View	2.33	0.07	[2.20, 2.46]	2.19	0.07	[2.05, 2.32]
Intensify	3.27	0.05	[3.16, 3.37]	3.23	0.06	[3.12, 3.35]

MRI data acquisition. MRI scans were conducted at University of Southern California's Dana and David Dornsife Cognitive Neuroimaging Center using a 3T Siemens MAGNETOM Prisma MRI scanner with a 32-channel head coil. We obtained a T1-weighted MPRAGE anatomic image (TR = 2300 ms, TE = 2.26 ms, slice thickness = 1.0 mm, flip angle = 9°, FOV = 256 mm, voxel size = 1.0 mm isotropic). We acquired 250 whole-brain volumes of T2*-weighted functional images using multi-EPI sequence (TR= 2400 mm, TE 18/35/53 ms, slice thickness = 3.0 mm, flip angle = 75°, FOV = 240 mm, voxel size = 3.0 mm isotropic).

Data analysis. The functional MRI (fMRI) data were denoised with ME-ICA, which removed artifact components using the linear echo-time dependence of BOLD signal changes (Kundu et al., 2012). The ME-ICA method allows robust data denoising for motion, physiological, and scanner artifacts via removal of non-BOLD components (Kundu et al., 2017).

The denoised data were entered into FMRI Expert Analysis Tool (FEAT), a tool of FMRIB Software Library (FSL) v6.0 (Jenkinson et al., 2012) for the individual- and group-level analysis. Individual-level analysis (Woolrich et al., 2001) included two steps of affine linear transformation with 12 degrees of freedom where each functional image was

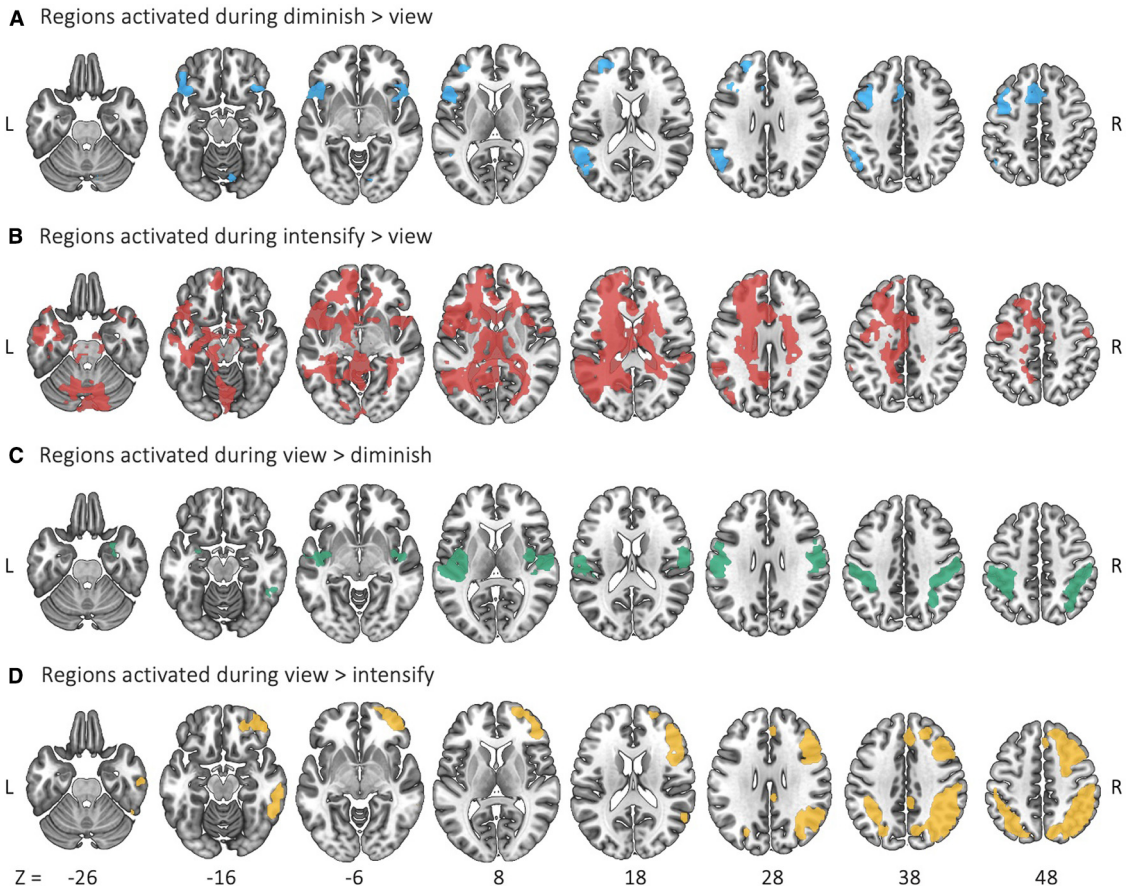

Figure 4. Regions showing activation differences between view and regulation conditions. ***A***, Areas (blue) that increased activity during downregulation. ***B***, Areas (red) that increased activity during upregulation. ***C***, Areas (green) in which activity was decreased during downregulation. ***D***, Areas (yellow) in which activity was decreased during upregulation.

registered to the MNI 152 T1 2-mm template via its T1-weighted anatomic image. Individual-level analysis also included a preprocessing of motion correction, spatial smoothing with 5-mm FWHM, and high-pass filtering with 600-s cutoff. Individual whole-brain BOLD time series were modeled with a linear combination of seven emotion-regulation regressors during the 6-s emotion regulation period (diminish-negative, view-negative, intensify-negative, diminish-positive, view-positive, intensify-positive, and view-neutral) along with their temporal derivatives, each convolved with a double-gamma hemodynamic response function. For the group-level analysis, FSL's mixed-effects model (FLAME 1) (Woolrich et al., 2004) was used to test the mean effect of emotion regulation effort, contrasted across the conditions. The final results were corrected for family-wise error at $p < 0.05$ with the cluster-wise threshold at $z > 3.1$. We tested for overlapping control regions by taking the intersection of intensify > view and diminish > view and tested the affective dial hypothesis by taking the intersection of intensify > view and view > diminish.

To characterize the nature of the brain areas identified by the view > diminish and intensify > view contrasts, we used emotion-associated and interoception-associated cluster maps from a meta-analytic study (Adolfi et al., 2017). This prior meta-analysis provided cluster maps for interoception, social cognition, and emotion. To help classify the brain regions activated during upregulation and downregulation, we derived three maps from the Adolfi et al. (2017) results: (1) the intersection of the two meta-analytic maps; (2) the emotion-associated map with the intersection regions removed; and (3) the interoception-associated map with the intersection regions removed. We then overlapped these three maps with the thresholded view > diminish and intensify > view contrast maps (after removing the intersection of diminish > view and intensify > view to remove activity likely related to regulation effort rather than its effects),

Table 2. Regions (Fig. 4*A*) that increased activity during downregulation (diminish > view)

Diminish > view clusters (Harvard-Oxford Structural Atlas)	MNI coordinate				
	x	*y*	*z*	z_{max}	Voxels
Supplementary motor cortex	−2	6	60	5.96	221
Paracingulate gyrus	−2	14	50	5.36	202
Angular gyrus	−58	−54	20	5.24	153
Superior frontal gyrus	−4	12	58	5.23	230
Frontal pole	−26	50	32	4.99	445
Cerebellum right crus I	36	−64	−38	4.99	212
Middle frontal gyrus	−46	14	38	4.89	291
Frontal operculum cortex	−44	18	0	4.88	70
Frontal orbital cortex	−38	20	−14	4.74	335
Inferior frontal gyrus, pars opercularis	−50	12	4	4.68	116
Lateral occipital cortex, superior division	−48	−64	40	4.63	194
Cerebellum right crus II	20	−72	−38	4.49	181
Supramarginal gyrus, posterior division	−60	−48	24	4.46	86
Cingulate gyrus, anterior division	−4	20	34	4.17	52
Inferior frontal gyrus, pars triangularis	−54	24	8	4.15	14
Insular cortex	−40	16	−2	3.91	34
Precentral gyrus	−44	−4	54	3.83	13
Cerebellum right VI	10	−76	−18	3.76	23
Lateral occipital cortex, inferior division	−54	−66	12	3.64	5
Lingual gyrus	12	−76	−10	3.55	20
Cerebellum right VIIb	18	−70	−42	3.37	3
Temporal pole	−44	18	−18	3.32	3

Cluster names are based on the Harvard-Oxford cortical and subcortical structural atlases in FSL (https://fsl.fmrib.ox.ac.uk/fsl/fslwiki/Atlases) with 50% minimum probability.

Table 3. Regions (Fig. 4*B*) that increased activity during upregulation (intensify > view)

Intensify > view clusters (Harvard-Oxford Structural Atlas)	MNI coordinate				
	x	*y*	*z*	z_{max}	Voxels
Left thalamus	−2	−22	6	7.38	938
Insular cortex	−38	4	2	7.11	366
Cingulate gyrus, anterior division	−2	14	34	7.09	877
Cerebellum right crus I	30	−76	−36	6.68	1129
Brainstem	−2	−32	−4	6.66	537
Left hippocampus	−30	−36	−4	6.62	271
Superior frontal gyrus	−12	−2	70	6.43	109
Central opercular cortex	−42	6	2	6.41	324
Cerebellum right crus II	30	−76	−38	6.39	875
Frontal operculum cortex	−44	24	0	6.36	119
Supplementary motor cortex	4	0	68	6.28	498
Right thalamus	2	−8	6	6.28	468
Precentral gyrus	54	0	44	6.20	297
Temporal pole	−48	18	−16	6.18	538
Lateral occipital cortex, superior division	−46	−72	24	6.15	317
Frontal orbital cortex	−44	24	−6	6.04	184
Supramarginal gyrus, posterior division	−58	−46	22	6.00	76
Left caudate	−16	−8	20	5.95	373
Cerebellum right V	2	−62	−6	5.91	47
Left lateral ventricle	−14	24	4	5.87	733
Left pallidum	−12	4	−4	5.87	102
Cerebellum vermis VI	0	−70	−18	5.81	216
Frontal pole	−30	44	24	5.81	1466
Cerebellum left I-IV	−6	−50	−6	5.80	189
Right lateral ventricle	10	−4	18	5.73	560
Cerebellum left crus I	−42	−56	−40	5.68	518
Cerebellum left V	0	−60	−6	5.65	184
Right caudate	18	−6	24	5.64	194
Left putamen	−30	4	4	5.50	400
Angular gyrus	−54	−54	18	5.43	96
Right hippocampus	32	−36	−6	5.37	105
Middle temporal gyrus, anterior division	−54	−4	−28	5.28	88
Left accumbens	−6	12	−4	5.27	53
Precuneus cortex	−14	−58	18	5.26	373
Cingulate gyrus, posterior division	−4	−54	28	5.26	197
Cerebellum right I-IV	2	−46	−6	5.21	49
Lingual gyrus	−10	−52	−4	5.17	213
Parahippocampal gyrus, posterior division	−18	−26	−20	5.16	28
Cerebellum right VI	8	−74	−22	5.15	252
Parietal operculum cortex	−34	−30	20	5.01	130
Middle frontal gyrus	−34	30	44	4.95	171
Cerebellum right VIIb	18	−72	−46	4.92	83
Inferior frontal gyrus, pars opercularis	−50	12	4	4.86	113
Frontal medial cortex	−6	54	−10	4.82	64
Cerebellum right VIIIb	14	−42	−54	4.81	15
Planum polare	−54	2	−2	4.81	31
Cerebellum left VI	−14	−62	−26	4.78	281
Cerebellum left crus II	−42	−56	−44	4.73	100
Right putamen	18	10	−8	4.73	66
Planum temporale	−60	−36	16	4.67	31
Paracingulate gyrus	−4	18	38	4.67	207
Middle temporal gyrus, temporo-occipital part	−60	−56	2	4.67	130
Temporal fusiform cortex, posterior division	−40	−34	−20	4.66	72
Lateral occipital cortex, inferior division	−54	−64	10	4.62	81
Left amygdala	−14	−6	−16	4.61	84
Subcallosal cortex	−2	12	−4	4.57	54
Temporal occipital fusiform cortex	34	−46	−8	4.56	14
Cerebellum right IX	6	−50	−52	4.52	29
Cerebellum right VIIIa	36	−52	−52	4.51	43
Occipital pole	−8	−96	2	4.37	59
Cerebellum vermis IX	2	−52	−32	4.34	12
Superior temporal gyrus, posterior division	66	−30	14	4.28	27
Parahippocampal gyrus, anterior division	−18	−20	−24	4.07	25
Cerebellum vermis X	2	−50	−34	4.02	7
Cerebellum left IX	−12	−46	−52	3.99	13
Middle temporal gyrus, posterior division	−64	−42	−10	3.96	11
Intracalcarine cortex	−6	−68	12	3.87	13
Cerebellum left X	−22	−40	−44	3.85	14
Right amygdala	16	−8	−18	3.80	26
Inferior frontal gyrus, pars triangularis	−52	24	−2	3.79	19
Occipital fusiform gyrus	28	−72	−8	3.77	11
Cerebellum vermis VIIIa	2	−72	−42	3.72	7
Right accumbens	10	10	−8	3.54	17
Inferior temporal gyrus, anterior division	−48	−2	−34	3.37	2
Cerebellum left VIIIa	−30	−44	−48	3.35	5
Postcentral gyrus	−22	−38	62	3.31	4
Cerebellum vermis Crus II	0	−78	−30	3.30	2
Supramarginal gyrus, anterior division	−64	−38	28	3.29	3
Cerebellum left VIIIb	−24	−40	−50	3.28	11
Superior temporal gyrus, anterior division	−58	2	−6	3.23	1

counted the number of voxels overlapping each of the three meta-analytic maps, and divided the number of overlapping voxels with the total number of voxels in each thresholded contrast map.

To assess the BOLD activity changes in the amygdala, we individually segmented the amygdala region from each participant's T1-weighted image using FreeSurfer version 6 (Fischl et al., 2002, 2004) and created the left and right amygdala masks in the native space. We then applied FSL FLIRT (Jenkinson and Smith, 2001; Jenkinson et al., 2002) to transform the masks to the standard MNI space and input them to Featquery to obtain average percent signal change values in the amygdala activity during emotion regulation.

We analyzed participants' ratings of their emotional intensity during the task using SPSS 22 (IBM) to conduct an ANOVA with mean emotional intensity as the dependent variable and the regulation goals (diminish, intensify, view) and image valence (negative, positive) as within-subject independent factors.

Finally, we examined how brain activity while implementing different regulation goals relates to subjective sense of emotional intensity. For this, we used the participants' rating scores on emotional intensity, ranging from 1 to 4. However, to compare the strength of the relationship between subjective emotional intensity and regional brain activity for the two regulation goals, we needed to normalize each participant's ratings within each regulation goal condition. In other words, for this question, the overall main effect of condition (intensify vs diminish) on emotional intensity was irrelevant. Instead, we wanted to see which brain regions showed activity that was associated with within-condition variation in emotional intensity and whether the brain regions showing such relationships differed across intensify and diminish conditions. To extract within-subject variations for the two conditions, we normalized the raw rating scores separately within each subject's intensify and diminish conditions by demeaning the rating scores and dividing the demeaned scores by the SD for each condition. The normalized scores for intensify and diminish trials were used as a weight for the two emotion-regulation regressors (diminish, intensify; each aggregated across positive and negative valence) in another individual-level analysis. Data preprocessing methods remained the same as in prior analyses. The subsequent group-level analysis using FSL's FLAME1 tested the mean effect of four contrasts: diminish, intensify, diminish > intensify, and intensify > diminish, and the results were corrected for family-wise error at $p < 0.05$ with the cluster-wise threshold at $z > 3.1$. We excluded 9 participants who always responded with the same rating within either condition, which made normalization impossible within that condition for that person.

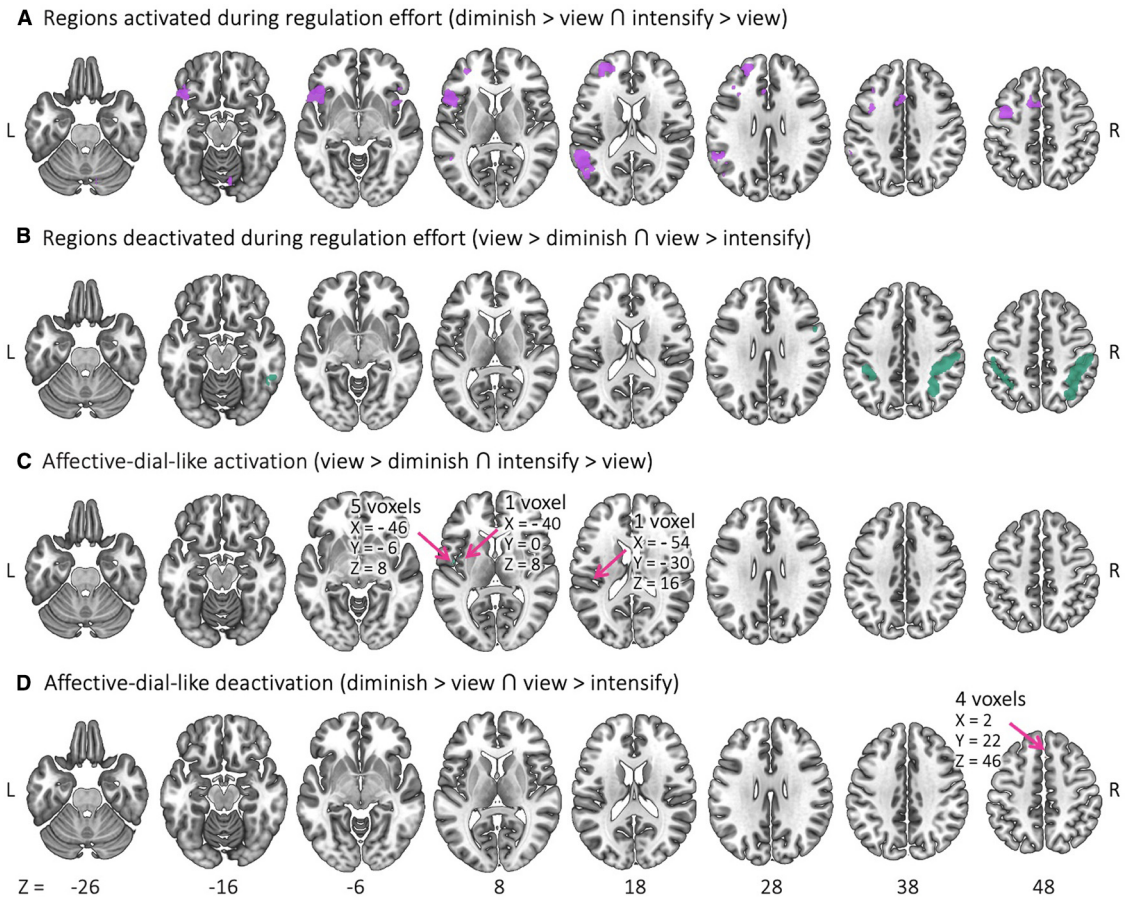

Figure 5. Brain activity consistent with regulatory effort versus with emotional outcome across regulation conditions. ***A***, Common regions (purple) activated during both upregulation and downregulation. ***B***, Regions (green) deactivated during both upregulation and downregulation. ***C***, Regions (turquoise) that increased activity during upregulation and decreased activity during downregulation. ***D***, Regions (orange) that decreased activity during upregulation and increased activity during downregulation.

Table 4. Regions (Fig. 4*C*) which decreased activity during down-regulation (view > diminish)

View > diminish clusters (Harvard-Oxford Structural Atlas)	MNI coordinate				
	x	y	z	Z_{max}	Voxels
Insular Cortex	−40	−6	8	6.38	352
Superior Parietal Lobule	−36	−50	60	5.92	363
Postcentral Gyrus	−42	−32	60	5.75	761
Supramarginal Gyrus, anterior division	−52	−32	44	5.74	175
Central Opercular Cortex	−42	−8	10	5.26	252
Precentral Gyrus	−58	4	28	5.13	124
Heschl's Gyrus including H1 and H2	−46	−24	12	5.08	111
Supramarginal Gyrus, posterior division	50	−38	54	4.88	18
Planum Temporale	−52	−28	10	4.70	77
Planum Polare	48	−8	−6	4.69	57
Lateral Occipital Cortex, superior division	32	−64	44	4.46	236
Parietal Operculum Cortex	−50	−28	14	4.41	49
Inferior Temporal Gyrus, temporo-occipital part	54	−48	−20	4.02	92
Right Amygdala	28	0	−22	3.97	39
Right Hippocampus	30	−6	−26	3.66	4
Left Amygdala	−28	−4	−16	3.63	16
Superior Temporal Gyrus, posterior division	60	−18	−2	3.47	2
Right Putamen	32	−10	6	3.44	2
Temporal Pole	28	6	−28	3.38	10
Parahippocampal Gyrus, anterior division	22	4	−32	3.38	5

Table 5. Regions (Fig. 4*D*) which decreased activity during up-regulation (view > intensify)

View > intensify clusters (Harvard-Oxford Structural Atlas)	MNI coordinate				
	x	y	z	Z_{max}	Voxels
Lateral Occipital Cortex, superior division	40	−60	46	9.24	1969
Angular Gyrus	48	−56	48	7.77	420
Frontal Pole	42	52	−12	7.31	1725
Middle Frontal Gyrus	36	16	52	7.18	439
Supramarginal Gyrus, posterior division	50	−44	50	7.15	119
Precentral Gyrus	54	10	24	6.39	50
Inferior Temporal Gyrus, posterior division	62	−28	−22	6.35	14
Superior Frontal Gyrus	24	24	56	6.33	157
Inferior Temporal Gyrus, temporo-occipital part	62	−44	−18	6.04	163
Superior Parietal Lobule	42	−46	56	6.03	119
Middle Temporal Gyrus, posterior division	66	−24	−18	6.00	94
Inferior Frontal Gyrus, pars opercularis	54	12	22	5.92	64
precuneus Cortex	8	−72	44	5.85	72
Paracingulate Gyrus	2	28	42	5.46	230
Supramarginal Gyrus, anterior division	54	−32	46	5.42	99
Postcentral Gyrus	54	−22	46	5.21	104
Cingulate Gyrus, posterior division	4	−36	32	5.17	148
Middle Temporal Gyrus, temporo-occipital part	64	−42	−10	4.22	17
Inferior Frontal Gyrus, pars triangularis	54	30	16	4.02	3
Frontal Orbital Cortex	20	32	−20	3.83	4

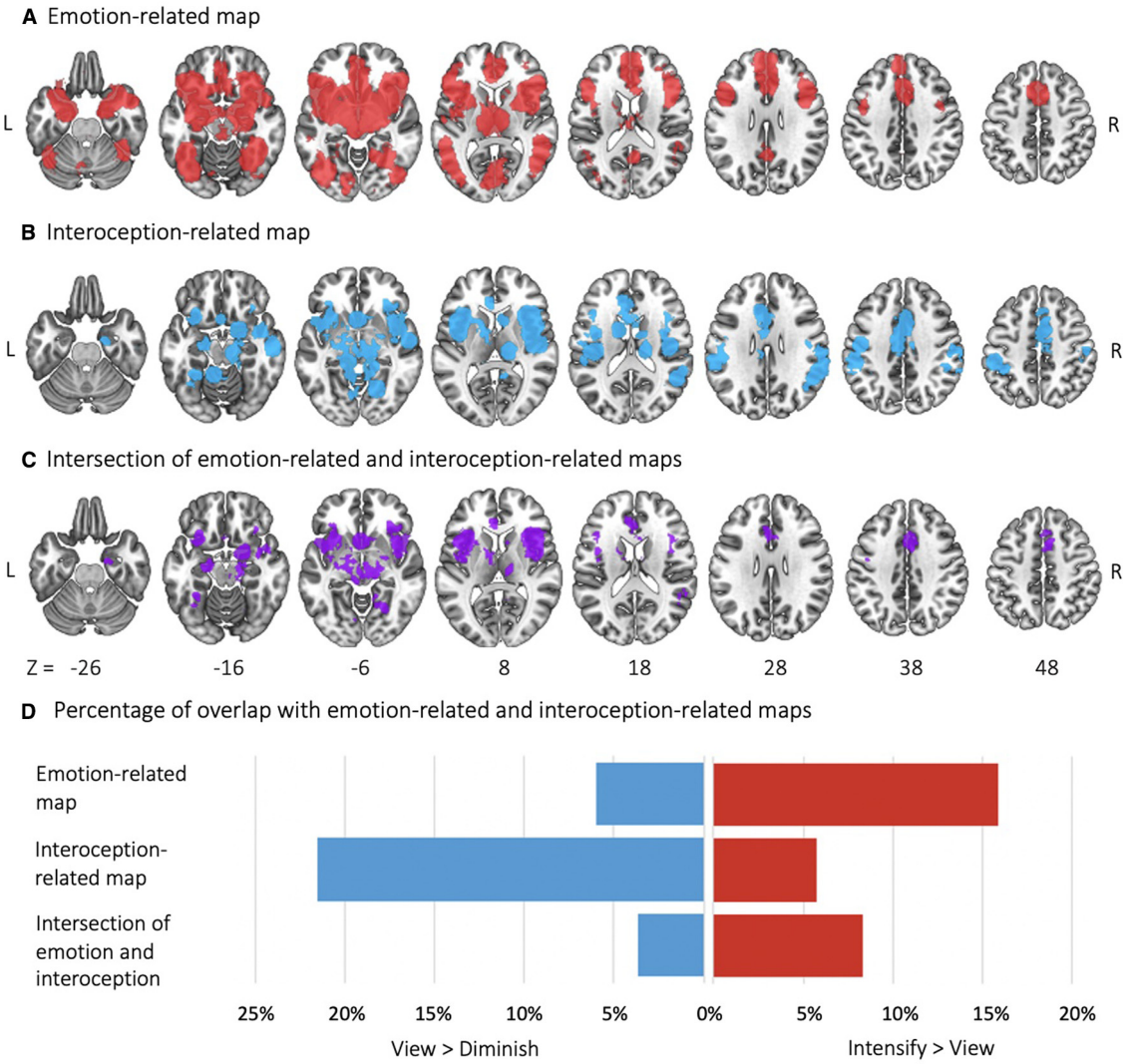

Figure 6. Emotion-related and interoception-related areas identified in the Adolfi et al. (2017) meta-analysis. While clusters (red) in ***A*** are related to emotion, clusters (blue) in ***B*** are related to interoception. ***C***, Intersection (purple) of ***A*** and ***B***. ***D***, Percentage of the voxels during downregulation and upregulation (Fig. 4*B*, *C*), which overlap with ***A***, ***B***, and ***C***.

Results

Self-rated emotional intensity

There was a significant main effect of the three emotion regulation goals ($F_{(2,208)} = 228.60$, $r = 0.83$, $p < 0.001$) and of emotional valence ($F_{(1,104)} = 5.58$, $r = 0.23$, $p = 0.02$) on self-rated emotional intensity. But there was no significant interaction between goals and valence ($F_{(2,208)} = 1.73$, $r = 0.13$, $p = 0.18$). We also conducted Bonferroni-corrected t tests for pairs of regulation and valence types. The corrected p threshold was at 0.007. Subjective intensity ratings were higher for intensifying than for viewing ($t_{(104)} = 12.68$, $r = 0.61$, $p < 0.001$ for negative emotion and $t_{(104)} = 16.19$, $r = 0.63$, $p < 0.001$ for positive emotion), and also higher for viewing than for diminishing ($t_{(104)} = 5.44$, $r = 0.29$, $p < 0.001$ for negative emotion and $t_{(104)} = 5.09$, $r = 0.25$, $p < 0.001$ for positive emotion) (Fig. 3). Ratings did not significantly differ between negative and positive emotion for intensifying ($t_{(104)} = 0.60$, $r = 0.03$, $p = 0.55$), diminishing ($t_{(104)} = 2.43$, $r = 0.09$, $p = 0.02$), or viewing, ($t_{(104)} = 2.46$, $r = 0.10$, $p = 0.02$), although the comparisons were significant at an uncorrected level for diminishing and viewing (Table 1). In addition, we found that participants' average ratings of emotional intensity during the task correlated with their confidence levels for each goal after the task: $r_{(103)} = -0.19$, $p = 0.06$ for diminishing negative emotion, $r_{(103)} = -0.29$, $p = 0.003$ for diminishing positive emotion, $r_{(103)} = 0.41$, $p < 0.001$ for intensifying negative emotion, and $r_{(103)} = 0.40$, $p < 0.001$ for intensifying positive emotion. All the correlations appeared to be goal-consistent as they were negative for downregulation and positive for upregulation.

Brain activity associated with regulation effort

Our analyses focused on the general regulatory effect of emotion regulation across positive and negative valence, based on prior findings that the brain's affective workspace varies little across valence (Lindquist et al., 2016). Contrasting the diminish against view condition (diminish > view) revealed brain regions showing increased activation during emotional downregulation (Fig. 4*A*; Table 2) (Desikan et al., 2006): the anterior insular cortex, lateral frontal orbital cortex, dorsal ACC, paracingulate gyrus, superior frontal gyrus, and inferior frontal gyrus (IFG). Contrasting the intensify against view condition (intensify > view) revealed brain regions showing increased activation during emotional upregulation (Fig. 4*B*; Table 3): the anterior insular

cortex, lateral frontal orbital cortex, frontal medial cortex, ACC, posterior cingulate gyrus, IFG, middle frontal gyrus, superior frontal gyrus, hippocampus, amygdala, putamen, and thalamus. There were a number of brain regions activated during both upregulation and downregulation (intensify > view ∩ diminish > view), consistent with regulatory regions shared by the two opposing regulation goals. These regions were the insular cortex, IFG, middle frontal gyrus, superior frontal gyrus, dorsal ACC, and angular gyrus (Fig. 5*A*).

To test the affective dial hypothesis, we examined the intersection of the two contrasts (intensify > view and view > diminish) that should show significant emotion-related activity if emotion regulation modulates affect-generating brain regions in the expected linear fashion (intensify > view > diminish). If emotion regulation processes act on the same affect-generating brain regions when upregulating and downregulating, the intensify > view and view > diminish contrasts should show overlapping areas. Despite our robust power, however, there were only seven voxels that were significant for both the intensify > view and view > diminish contrasts. They were in the central opercular cortex (five voxels), the parietal operculum cortex (one voxel), and the insular cortex (one voxel). Besides these seven voxels (Fig. 5*C*), there was no overlap between the significant clusters in the two contrasts, suggesting that upregulation and downregulation act on two distinct emotion-generating regions. The intensify > view contrast (Fig. 4*B*; Table 3) revealed the amygdala, striatum, anterior insular cortex, and cingulate gyrus, which are associated with emotional experience (Lindquist et al., 2016), as well as white matter and ventricular regions, which are associated with vascular activity during sympathetic arousal (Özbay et al., 2019). The view > diminish contrast (Fig. 4*C*; Table 4) showed the posterior insular cortex and postcentral gyrus, which receive visceral and sensory input and represent the physiological states of the body (Craig, 2002). The regions with lowered activity during intensifying emotion (view > intensify) included the frontal pole, middle frontal gyrus, and angular gyrus (Fig. 4*D*; Table 5). Similarly, examining the diminish > view and view > intensify intersection revealed only 4 voxels in the paracingulate gyrus, consistent with a linear diminish > view > intensify affective dial suppression pattern (Fig. 5*D*).

In addition, we tested whether the view > diminish and intensify > view contrasts differed between positive and negative valence conditions. We found no significant clusters except for one in the left angular gyrus (Z_{max} = 4.13; x_{max} = −48, y_{max} = −58, z_{max} = 44; 151 voxels) during view > diminish for negative compared with positive emotion. We also checked whether an affective dial pattern would emerge within either positive or negative trials analyzed separately. Neither the intersection of intensify > view and view > diminish contrasts nor the intersection of diminish > view and view > intensify contrasts yielded any significant voxels that overlapped when we analyzed positive and negative trials separately.

The lack of much activity consistent with either an intensify > view > diminish or a diminish > view > intensify pattern suggests that intensifying and diminishing emotions target different brain networks to modulate emotion. To help characterize the nature of the brain regions which emotion upregulation versus downregulation act on, we counted how many voxels activated during intensify > view versus view > diminish overlapped with emotion- versus interoception-associated cluster maps generated from a prior meta-analysis (Adolfi et al., 2017) (for maps, see Fig. 6). We found that 21.5% of activated voxels during view > diminish overlapped with interoception-related areas, while only 6.0% overlapped with emotion-related areas. During intensify > view, 15.9% overlapped emotion-related areas, while 5.7% overlapped interoception-related areas.

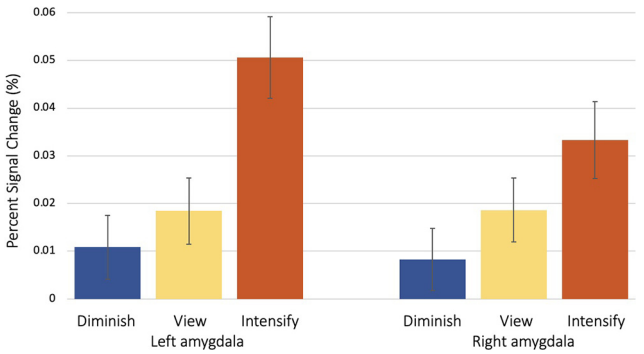

Figure 7. Activity in the amygdala ROIs during downregulation, viewing, and upregulation. Error bars indicate SE of each condition.

Table 6. Activity difference in amygdala ROI between regulation and view conditions[a]

Contrast	Mean	SE	*t*	df	*p*	95% CI
Left amygdala						
Intensify > view	0.032	0.008	4.118	104	<0.001	[0.017, 0.048]
View > diminish	0.008	0.006	1.202	104	0.232	[−0.005, 0.020]
Right amygdala						
Intensify > view	0.015	0.007	2.035	104	0.044	[0.0004, 0.029]
View > diminish	0.010	0.006	1.665	104	0.099	[−0.002, 0.023]

[a]Pairwise comparisons were performed on percent signal change values between conditions.

In our follow-up ROI analysis, although the amygdala numerically showed the affective-dial-like diminish < view < intensify pattern (Fig. 7), neither the right or left amygdala showed both significant diminish < view and view < intensify effects as predicted by the affective dial hypothesis. A *post hoc t* test with Bonferroni-corrected *p* threshold at 0.01 showed that activity in the left amygdala differed between intensify and view ($t_{(104)}$ = 4.12, r = 0.20, p < 0.001) but did not differ significantly between view and diminish ($t_{(104)}$ = 1.20, r = 0.05, p = 0.23). Activity in the right amygdala did not differ significantly between intensify and view ($t_{(104)}$ = 2.04, r = 0.10, p = 0.04), nor between view and diminish ($t_{(104)}$ = 1.67, r = 0.08, p = 0.10), but differed between intensify and view at an uncorrected *p* threshold (Table 6).

Brain activity associated with the subjective sense of regulation outcome

Our findings that upregulation and downregulation effort modulated mostly nonoverlapping affect-generating regions (Fig. 4*B*, *C*) raised the question of whether brain regions contributing to participants' sense of emotional intensity differ during upregulation and downregulation. The normalized rating scores within subjects for the diminish or intensify condition weighted each trial based on how extreme each participant's intensity rating was on that trial compared with the average rating for diminishing or intensifying trials. The SD of raw rating scores did not significantly differ between intensifying and diminishing trials ($t_{(95)}$ = 1.125, r = 0.06, p = 0.26), indicating similar variability in emotional intensity in the two conditions.

We first examined brain regions where activity during the 6-s task period (Fig. 2) was positively associated with subjective

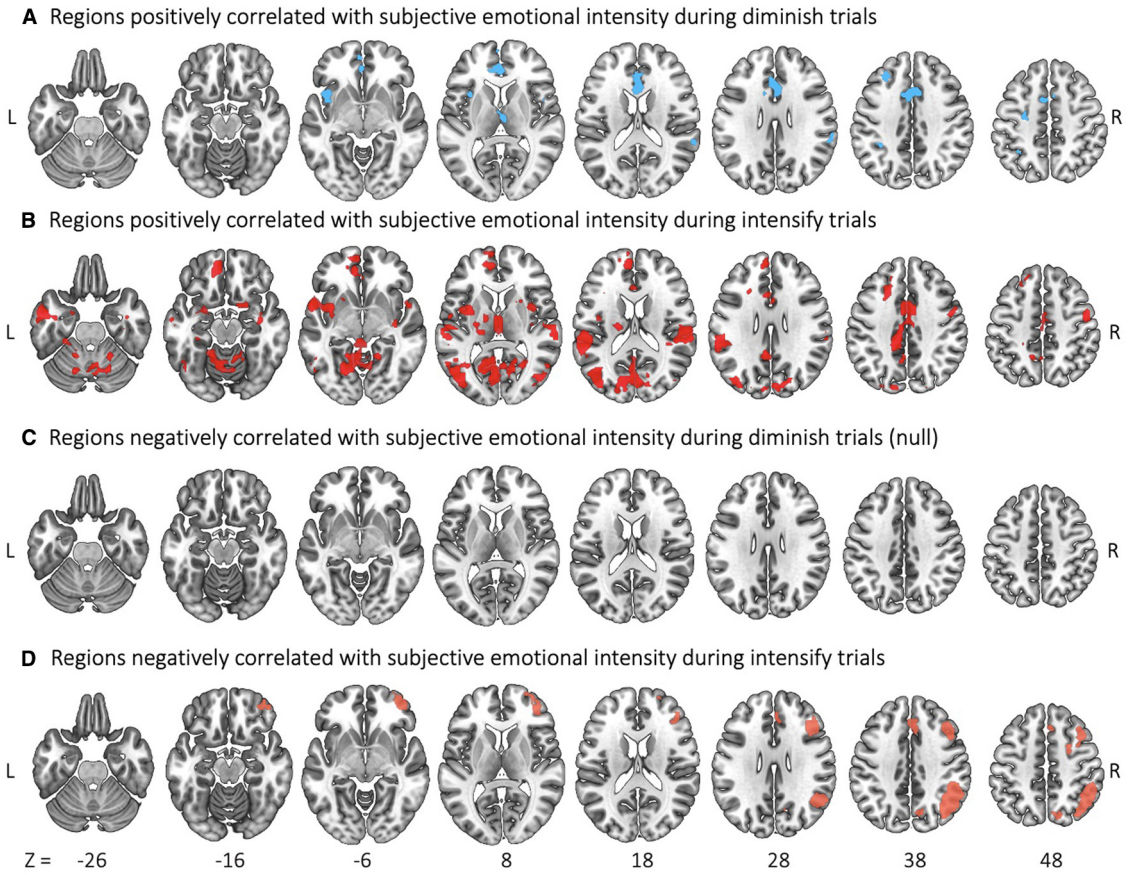

Figure 8. Regions correlated with subjective emotional intensity during diminish or intensify trials. ***A***, Regions (blue) that increased activity as subjective emotional intensity increased during diminish trials. ***B***, Regions (red) that increased activity as subjective emotional intensity increased during intensify trials. ***C***, Regions (null) that increased activity as subjective emotional intensity decreased during diminish trials. ***D***, Regions (orange) that decreased activity as subjective emotional intensity increased during intensify trials.

sense of emotional intensity separately for each condition. While higher subjective emotional intensity after diminishing was associated with the ACC and paracingulate gyrus (Fig. 8*A*; Table 7), subjective emotional intensity after intensifying was associated with broader areas, including the dorsal ACC, supplementary motor cortex, lingual gyrus, thalamus, and cerebellum (Fig. 8*B*; Table 8). The dorsal ACC, insula, thalamus, and frontal pole were overlapping areas that were associated with greater subjective emotional intensity across both intensifying and diminishing conditions (Fig. 9*A*). We then examined whether there were any brain regions in which activity was negatively associated with subjective emotional intensity. There were no significant regions for the diminish condition (Fig. 8*C*); but in the intensify condition, there was less activity in right frontoparietal regions during trials with higher subjective emotional intensity (Fig. 8*D*; Table 9).

The intersection of Figure 8*A* and 8*B* revealed that, during both upregulation and downregulation, participants reported greater feeling intensity when activation in the insula, ACC, and thalamus was higher (Fig. 9*A*). In contrast, the intersection of Figure 8*A* and 8*D* reflects goal-inconsistent subjective emotional intensity in both conditions (i.e., higher feeling intensity during diminish trials and lower feeling intensity during intensify trials) and revealed a separate ACC region (Fig. 9*B*). There also were some significant differences across regulation conditions in how subjective emotional intensity was associated with brain activity. The diminish > intensify contrast revealed significant condition differences in the angular gyrus, supramarginal gyrus, dorsal ACC, paracingulate gyrus, and middle frontal gyrus (Fig. 9*C*). The intensify > diminish contrast revealed significant differences in the postcentral gyrus and superior parietal lobule (Fig. 9*D*). However, it is important to note that, in the diminish > intensify contrast, the differences across regulation conditions were driven by effects within the intensify condition, as the regions in Figure 9*C* overlap with those in Figure 8*D*, which indicates greater negative associations between frontoparietal regions and subjective emotional intensity during intensify than diminish trials. Thus, we did not find any evidence of regions that are

Table 7. Regions (Fig. 8*A*) that increased activity as subjective emotional intensity increased during diminish trials

Regions positively correlated with ratings during diminish	MNI coordinate				
	x	*y*	*z*	z_{max}	Voxels
Cingulate gyrus, anterior division	−2	28	24	4.97	618
Insular cortex	−34	12	4	4.88	135
Right thalamus	4	−6	0	4.50	78
Frontal operculum cortex	40	24	2	4.20	34
Middle frontal gyrus	−30	30	34	4.14	50
Paracingulate gyrus	6	18	38	4.13	82
Supramarginal gyrus, posterior division	64	−40	18	3.92	50
Supplementary motor cortex	−4	6	48	3.82	11
Frontal pole	−4	58	0	3.57	53
Left thalamus	0	−8	6	3.49	13
Supramarginal gyrus, anterior division	64	−30	30	3.48	2
Central opercular cortex	48	6	2	3.25	2
Frontal medial cortex	−4	54	−8	3.10	1

more associated with subjective intensity during diminishing than during intensifying emotions.

Discussion

The field of emotion regulation has an unexamined assumption we call the affective dial hypothesis. According to this hypothesis, exerting emotional control increases affect-generating brain regions' activity during emotion upregulation and decreases these regions' activity during emotion downregulation. However, our well-powered ($N = 105$) study demonstrated that upregulation and downregulation target separate brain regions. Most of the brain regions downregulated by diminishing did not overlap with those upregulated by intensifying emotions, as indicated by the minimal intersection between the intensify > view and view > diminish contrasts (Fig. 5*C*).

Compared with viewing pictures, upregulating emotion increased activity in many brain regions (Fig. 4*B*) previously associated with affective experience, including the amygdala, anterior insular cortex, ACC, thalamus, and nucleus accumbens as well as in regions associated with sympathetic vascular activity, such as periventricular white matter (Özbay et al., 2018). Instead of decreasing activity in these same brain regions as predicted by the affective dial hypothesis, downregulating emotion decreased activity in the posterior insular cortex and postcentral gyrus (Fig. 4*C*). These areas receive visceral information through the afferent vagus nerve and are involved in interoceptive awareness (Craig, 2002; Khalsa et al., 2009). Indeed, downregulating activated more brain regions linked by a previous meta-analysis (Adolfi et al., 2017) with interoception than brain regions associated with emotion experience, recognition, or perception, whereas upregulating showed the reverse pattern (Fig. 6*D*).

It is possible that different strategy preferences across upregulation and downregulation activated different affective circuits. When upregulating, participants may have engaged more with emotional images; previous studies indicate that personalizing stimuli activate emotional arousal pathways, such as the amygdala and hippocampus (Kim and Hamann, 2007; Sokołowski et al., 2021). On the other hand, during downregulating, participants may have disengaged emotions by rationalizing the external situation, thereby reducing activity in interoceptive processing pathways involving the insula and inferior parietal lobule (Ochsner et al., 2004). Consistent with differential strategy selection for intensifying versus diminishing, *post hoc* review of the strategies and examples reported by the participants revealed that, to diminish emotion, 74% of participants reported reframing the situation, whereas to intensify emotion, 70% of them reported minimizing the distance from the scene. However, future research is needed to test the effects of personalizing versus rationalizing as the post-study questions were not tailored to distinguish one subtype of reappraisal strategy from another and the answers did not indicate exclusive use of those strategies. Aggregating across positive and negative valence did not appear to play a role because we found few significant differences across valence in the two contrasts (view > diminish, intensify > view), suggesting similar effects across valence. However, we note that including both upregulation and downregulation conditions within subjects in our study might have led to different baseline brain activity compared with a between-subject design comparing these two regulatory goals.

Although the brain regions targeted by upregulation and downregulation barely overlapped (Fig. 5*C, D*), these regulatory

Table 8. Regions (Fig. 8*B*) that increased activity as subjective emotional intensity increased during intensify trials

Regions positively correlated with ratings during intensify	MNI coordinate				
	x	*y*	*z*	z_{max}	Voxels
Lateral occipital cortex, superior division	−42	−80	22	5.97	375
Planum temporale	−58	−34	16	5.84	102
Insular cortex	−36	0	8	5.62	209
Parietal operculum cortex	−58	−34	20	5.58	166
Left thalamus	0	−16	8	5.44	234
Cingulate gyrus, anterior division	0	4	38	5.40	497
Lingual gyrus	−8	−60	4	5.25	484
Right thalamus	2	−18	8	5.09	70
Central opercular cortex	46	4	2	4.98	161
Paracingulate gyrus	−8	50	6	4.81	175
Superior parietal lobule	−30	−48	58	4.79	186
Cingulate gyrus, posterior division	−4	−50	30	4.73	169
Intracalcarine cortex	−18	−66	8	4.73	209
Cerebellum left I-IV	−4	−52	−2	4.72	75
Temporal pole	−58	6	−6	4.67	93
Precentral gyrus	48	−4	50	4.66	127
Cerebellum right VI	20	−52	−22	4.59	176
Cuneal cortex	4	−82	20	4.55	88
Cerebellum left V	−8	−58	−12	4.55	323
Lateral occipital cortex, inferior division	−42	−72	12	4.53	298
Planum polare	−54	2	−2	4.51	25
Precuneus cortex	−8	−52	54	4.50	405
Cerebellum left VI	−6	−64	−12	4.50	227
Cerebellum right V	20	−52	−24	4.47	185
Supramarginal gyrus, posterior division	−60	−46	20	4.46	16
Cerebellum right crus I	46	−62	−36	4.39	99
Left putamen	−26	−14	10	4.38	66
Brainstem	−4	−36	−6	4.36	41
Left amygdala	−22	0	−22	4.35	51
Frontal pole	−6	58	−10	4.31	188
Cerebellum vermis VI	−4	−66	−14	4.29	72
Superior frontal gyrus	−6	52	28	4.28	11
Temporal fusiform cortex, posterior division	−26	−38	−22	4.19	48
Supracalcarine cortex	2	−76	18	4.15	13
Middle temporal gyrus, posterior division	−62	−14	−22	4.13	9
Postcentral gyrus	−30	−38	64	4.10	61
Superior temporal gyrus, posterior division	66	−30	14	4.08	20
Frontal medial cortex	−6	52	−14	4.07	40
Right putamen	24	12	4	4.04	60
Cerebellum right I-IV	10	−50	−10	3.87	31
Frontal orbital cortex	22	8	−18	3.84	25
Temporal occipital fusiform cortex	−22	−48	−14	3.84	4
Supplementary motor cortex	2	−10	58	3.84	155
Right caudate	10	10	0	3.83	4
Cerebellum vermis VIIIa	2	−62	−30	3.83	29
Middle temporal gyrus, anterior division	−62	−8	−18	3.82	42
Superior temporal gyrus, anterior division	−58	2	−6	3.82	3
Left lateral ventricle	−12	−18	22	3.76	10
Supramarginal gyrus, anterior division	−60	−30	28	3.76	35
Occipital pole	8	−90	26	3.64	3
Middle temporal gyrus, temporo-occipital part	−58	−60	8	3.61	10
Right amygdala	22	2	−22	3.61	11
Inferior temporal gyrus, temporo-occipital part	−48	−56	−16	3.57	9
Left caudate	−16	−16	22	3.48	1
Heschl's gyrus, including H1 and H2	50	−16	8	3.46	10
Right accumbens	8	8	−4	3.42	3
Parahippocampal gyrus, posterior division	−30	−32	−18	3.40	2
Parahippocampal gyrus, anterior division	−30	−10	−32	3.38	4
Right pallidum	22	−2	4	3.28	1
Right hippocampus	34	−14	−16	3.24	2

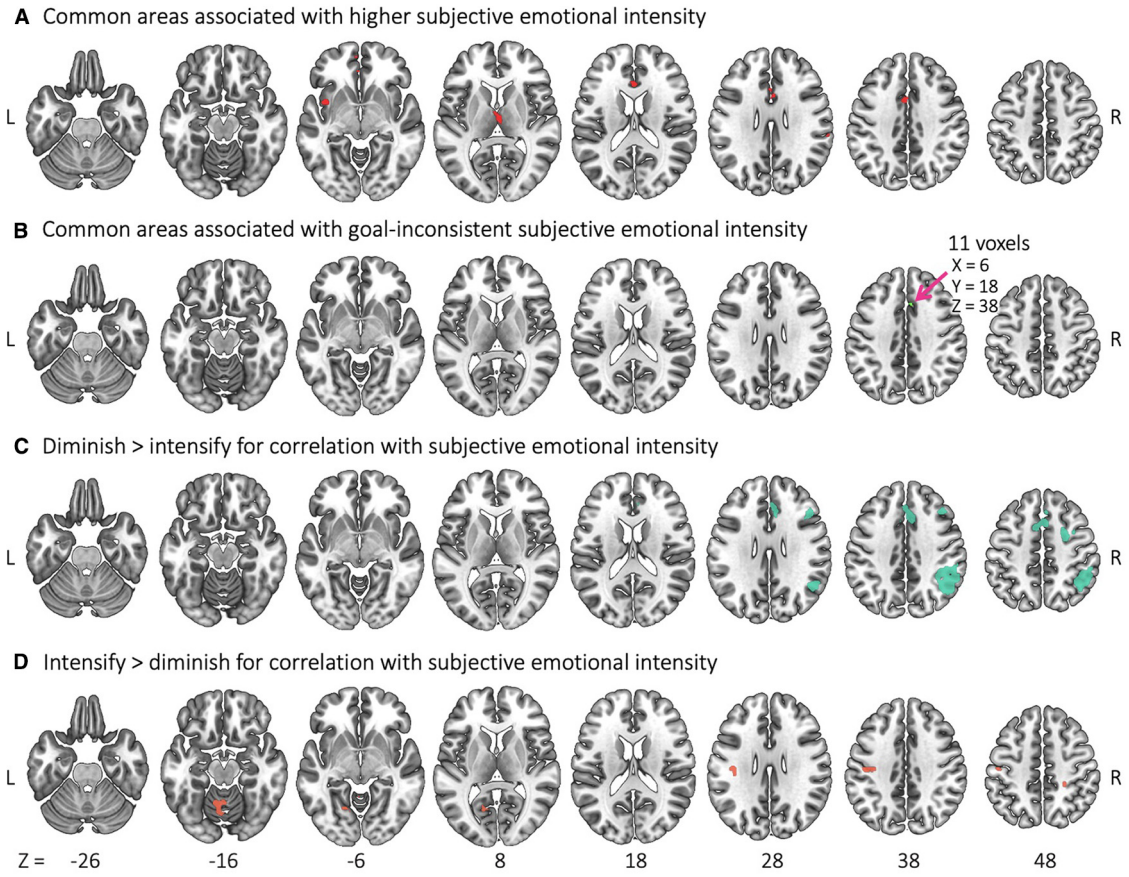

Figure 9. Similarities and differences between regulation conditions in the regions correlated with subjective emotional intensity. ***A***, The intersection (red) of regions positively correlated with subjective emotional intensity during diminish trials (see Fig. 8*A*) and during intensify trials (see Fig. 8*B*). ***B***, The intersection (mint) of regions positively correlated with subjective emotional intensity during diminish trials (see Fig. 8*A*) and regions negatively correlated with subjective emotional intensity during intensify trials (see Fig. 8*D*). ***C***, Regions (green) correlated with subjective emotional intensity more positively during diminish than intensify trials or more negatively during intensify than diminish trials. ***D***, Regions (orange) correlated with subjective emotional intensity more positively during intensify than diminish trials or more negatively during diminish than intensify trials.

Table 9. Regions (Fig. 8*D*) that decreased activity as subjective emotional intensity increased during intensify trials

Regions negatively correlated with ratings during intensify	MNI coordinate				
	x	*y*	*z*	z_{max}	Voxels
Angular gyrus	50	−56	42	6.43	321
Cingulate gyrus, anterior division	4	28	30	3.57	1
Frontal pole	40	56	2	6.11	646
Lateral occipital cortex, superior division	44	−64	42	6.21	487
Middle frontal gyrus	42	26	38	5.72	307
Paracingulate gyrus	4	26	44	5.14	276
Precuneus cortex	12	−68	32	4.56	55
Superior frontal gyrus	20	26	56	4.81	40
Supramarginal gyrus, posterior division	52	−44	46	5.42	67

modes activated an overlapping set of brain regions (Fig. 5*A*), including the IFG, dorsal ACC, and anterior insular cortex, regions associated with various aspects of emotion regulation (Ochsner et al., 2004; Eippert et al., 2007; Kim and Hamann, 2007; Domes et al., 2010; Li et al., 2018). Our participants used cognitive reappraisal strategies; the IFG, within the ventrolateral PFC, is involved in strategies that require modifying interpretations of emotional situations to attenuate negative emotion (Ochsner and Gross, 2005). The dorsal ACC detects conflicts and signals adjustments in cognitive tasks (Bush et al., 2000; Botvinick et al., 2004) and emotion regulation (McRae et al., 2008; Ichikawa et al., 2011; Etkin et al., 2015). Anterior insula activation is associated with subjective feelings of emotion and their autonomic representation (Craig, 2009; Critchley and Harrison, 2013).

The amygdala showed a linear pattern; its BOLD activity was highest during upregulation, mid-range during viewing, and lowest during downregulation (Fig. 7). This seemed to support prior work on how emotion regulation modulates amygdala activity (e.g., Ochsner et al., 2004; Kim and Hamann, 2007; Goldin et al., 2008; McRae et al., 2010; Steinfurth et al., 2018). However, to our knowledge, there are no prior findings of overlapping upregulation > baseline and baseline > downregulation effects in the amygdala at a whole-brain threshold level as prior findings were based on ROI or small-volume-corrected analyses. Likewise, we found no significant amygdala voxels in the affective-dial intensify > view ∩ view > diminish contrast at the whole-brain level with our conservative threshold (cluster size $Z > 3.1$). Participants' self-reported greater use of reframing during downregulation than upregulation may be relevant as reinterpretation does not tend to lower amygdala activity (Dörfel et al., 2014). Further examination of our whole-brain results showed that the view > diminish contrast activated amygdalar laterobasal subregions receiving sensory information, whereas the intensify > view contrast activated mostly the superficial and centromedial subregions, related to emotional arousal and responses (Kerestes et al., 2017). Future research should investigate whether upregulation and downregulation reliably target different amygdala subregions.

During each trial, participants rated the intensity of their feelings (Fig. 2). As expected, they rated intensity as lower on diminish than on intensify trials (Fig. 3). But does variation in subjective emotional intensity relate to activity in the same brain regions during upregulating versus downregulating emotion? Indeed, we found several brain regions where increased activity both during diminishing and intensifying emotions was associated with relatively greater subjective emotional intensity (Fig. 9*A*). These included the left insula (Fig. 9*A*) and a small cluster in the right insula (not shown). The insula's activity level may help signal emotional intensity as it is associated with both interoception and emotion (Fig. 6*C*) (Adolfi et al., 2017). Other regions whose activity was correlated with subjective emotional intensity included the dorsal ACC and the frontal pole, which, as part of the medial PFC, activate during self-referencing tasks involving emotional stimuli (Northoff et al., 2006).

There were also interesting differences across conditions. When the goal was to intensify emotions, higher subjective emotional intensity was associated with lower activity in the right frontoparietal attention network (e.g., Laird et al., 2011), suggesting that intensifying emotions suppresses activity in this attention network (Fig. 8*D*). Directly contrasting the correlations with subjective emotional intensity in the two conditions revealed that this suppression of frontoparietal activity was more associated with subjective emotional intensity during intensifying than during diminishing emotion (Fig. 9*C*, *D*). Thus, whereas amping up emotion during upregulation suppresses frontoparietal activity (Fig. 8*D*), tamping down emotion during downregulation does not increase frontoparietal activity (Fig. 8*C*). This suggests that subjective emotional intensity affects cognitive control abilities associated with the frontoparietal attention network more during upregulation than downregulation.

In contrast, activity in a dorsal ACC region (Fig. 9*B*) was associated with lower subjective intensity during intensify trials (i.e., a failure to achieve the instructed higher arousal state; Fig. 8*D*) and with higher subjective intensity ratings on diminish trials (i.e., again, a failure to achieve the instructed lower arousal state; Fig. 8*A*). This region appears to be providing a task-failure signal (or reflecting compensatory effort in response to failure), consistent with the role of the dorsal ACC in error monitoring (Taylor et al., 2007; Gilbertson et al., 2021). Thus, upregulation and downregulation appear to rely on some overlapping brain regions (Fig. 9*A-B*) to integrate arousal signals and to monitor the gap between the goal and actual states, despite the differences we identified in affect-generating brain regions targeted by these two regulatory goals.

We observed broad activation in the white matter surrounding the ventricles during intensifying emotion compared with viewing emotional images (Fig. 4*B*). Although we could not find prior papers mentioning white matter activation during emotion regulation, we observed it in figures depicting the fMRI results of emotion upregulation (e.g., Arbuckle and Shane, 2017, their Fig. 1; Grosse Rueschkamp et al., 2019, their Fig. 4). Increased white matter BOLD signal during upregulation may be caused by emotional arousal and sympathetic activity increasing vascular tone (Özbay et al., 2018). White matter veins converge to subependymal veins that run around the edge of the lateral ventricles (Okudera et al., 1999), and so periventricular white matter is especially susceptible to systemic changes in vascular tone (Özbay et al., 2018). Future studies should examine how autonomic nervous system activity affects the vascular aspect of BOLD signals during emotion regulation.

In conclusion, in the current study, cognitive reappraisal during upregulation versus downregulation activated an overlapping set of control regions and relied on an overlapping set of regions to inform subjective sense of emotional intensity but modulated distinct affect-generating brain regions. The regions targeted by upregulation were more likely to be involved in emotional arousal, whereas regions targeted by downregulation were more likely to be involved in interoception. These findings suggest that upregulating and downregulating our emotions using cognitive reappraisal target different affective circuits in the brain rather than exerting opposing effects on the same emotion-generating brain regions. This dissociation between targeted brain regions raises the possibility that some individuals may excel at upregulating but not at downregulating their own emotions, or vice versa.

References

Adolfi F, Couto B, Richter F, Decety J, Lopez J, Sigman M, Manes F, Ibáñez A (2017) Convergence of interoception, emotion, and social cognition: a twofold fMRI meta-analysis and lesion approach. Cortex 88:124–142.

Arbuckle NL, Shane MS (2017) Upregulation of neural indicators of empathic concern in an offender population. Soc Neurosci 12:386–390.

Botvinick MM, Cohen JD, Carter CS (2004) Conflict monitoring and anterior cingulate cortex: an update. Trends Cogn Sci 8:539–546.

Braunstein LM, Gross JJ, Ochsner KN (2017) Explicit and implicit emotion regulation: a multi-level framework. Soc Cogn Affect Neurosci 12:1545–1557.

Buhle JT, Silvers JA, Wager TD, Lopez R, Onyemekwu C, Kober H, Weber J, Ochsner KN (2014) Cognitive reappraisal of emotion: a meta-analysis of human neuroimaging studies. Cereb Cortex 24:2981–2990.

Bush G, Luu P, Posner MI (2000) Cognitive and emotional influences in anterior cingulate cortex. Trends Cogn Sci 4:215–222.

Craig AD (2002) How do you feel? Interoception: the sense of the physiological condition of the body. Nat Rev Neurosci 3:655–666.

Craig AD (2009) How do you feel–now? The anterior insula and human awareness. Nat Rev Neurosci 10:59–70.

Critchley HD, Harrison NA (2013) Visceral influences on brain and behavior. Neuron 77:624–638.

Desikan RS, Ségonne F, Fischl B, Quinn BT, Dickerson BC, Blacker D, Buckner RL, Dale AM, Maguire RP, Hyman BT, Albert MS, Killiany RJ (2006) An automated labeling system for subdividing the human cerebral cortex on MRI scans into gyral based regions of interest. Neuroimage 31:968–980.

Domes G, Schulze L, Böttger M, Grossmann A, Hauenstein K, Wirtz PH, Heinrichs M, Herpertz SC (2010) The neural correlates of sex differences in emotional reactivity and emotion regulation. Hum Brain Mapp 31:758–769.

Dörfel D, Lamke JP, Hummel F, Wagner U, Erk S, Walter H (2014) Common and differential neural networks of emotion regulation by detachment, reinterpretation, distraction, and expressive suppression: a comparative fMRI investigation. Neuroimage 101:298–309.

Eippert F, Veit R, Weiskopf N, Erb M, Birbaumer N, Anders S (2007) Regulation of emotional responses elicited by threat-related stimuli. Hum Brain Mapp 28:409–423.

Etkin A, Büchel C, Gross JJ (2015) The neural bases of emotion regulation. Nat Rev Neurosci 16:693–700.

Faul F, Erdfelder E, Lang AG, Buchner A (2007) G* Power 3: a flexible statistical power analysis program for the social, behavioral, and biomedical sciences. Behav Res Methods 39:175–191.

Fischl B, Salat DH, Busa E, Albert M, Dieterich M, Haselgrove C, van der Kouwe A, Killiany R, Kennedy D, Klaveness S, Montillo A, Makris N, Rosen B, Dale AM (2002) Whole brain segmentation: automated labeling of neuroanatomical structures in the human brain. Neuron 33:341–355.

Fischl B, van der Kouwe A, Destrieux C, Halgren E, Ségonne F, Salat DH, Busa E, Seidman LJ, Goldstein J, Kennedy D, Caviness V, Makris N, Rosen B, Dale AM (2004) Automatically parcellating the human cerebral cortex. Cereb Cortex 14:11–22.

Gilbertson H, Fang L, Andrzejewski JA, Carlson JM (2021) Dorsal anterior cingulate cortex intrinsic functional connectivity linked to electrocortical measures of error monitoring. Psychophysiology 58:e13794.

Goldin PR, McRae K, Ramel W, Gross JJ (2008) The neural bases of emotion regulation: reappraisal and suppression of negative emotion. Biol Psychiatry 63:577–586.

Gross JJ (2015) Emotion regulation: current status and future prospects. Psychol Inquiry 26:1–26.
Grosse Rueschkamp JM, Brose A, Villringer A, Gaebler M (2019) Neural correlates of upregulating positive emotions in fMRI and their link to affect in daily life. Soc Cogn Affect Neurosci 14:1049–1059.
Ichikawa N, Siegle GJ, Jones NP, Kamishima K, Thompson WK, Gross JJ, Ohira H (2011) Feeling bad about screwing up: emotion regulation and action monitoring in the anterior cingulate cortex. Cogn Affect Behav Neurosci 11:354–371.
Jenkinson M, Bannister P, Brady M, Smith S (2002) Improved optimization for the robust and accurate linear registration and motion correction of brain images. Neuroimage 17:825–841.
Jenkinson M, Beckmann CF, Behrens TE, Woolrich MW, Smith SM (2012) FSL. Neuroimage 62:782–790.
Jenkinson M, Smith S (2001) A global optimisation method for robust affine registration of brain images. Med Image Anal 5:143–156.
Kerestes R, Chase HW, Phillips ML, Ladouceur CD, Eickhoff SB (2017) Multimodal evaluation of the amygdala's functional connectivity. Neuroimage 148:219–229.
Khalsa SS, Rudrauf D, Feinstein JS, Tranel D (2009) The pathways of interoceptive awareness. Nat Neurosci 12:1494–1496.
Kim SH, Hamann S (2007) Neural correlates of positive and negative emotion regulation. J Cogn Neurosci 19:776–798.
Kohn N, Eickhoff SB, Scheller M, Laird AR, Fox PT, Habel U (2014) Neural network of cognitive emotion regulation: an ALE meta-analysis and MACM analysis. Neuroimage 87:345–355.
Kundu P, Inati SJ, Evans JW, Luh WM, Bandettini PA (2012) Differentiating BOLD and non-BOLD signals in fMRI time series using multi-echo EPI. Neuroimage 60:1759–1770.
Kundu P, Voon V, Balchandani P, Lombardo MV, Poser BA, Bandettini PA (2017) Multi-echo fMRI: a review of applications in fMRI denoising and analysis of BOLD signals. Neuroimage 154:59–80.
Laird AR, Fox PM, Eickhoff SB, Turner JA, Ray KL, McKay DR, Glahn DC, Beckmann CF, Smith SM, Fox PT (2011) Behavioral interpretations of intrinsic connectivity networks. J Cogn Neurosci 23:4022–4037.
Leiberg S, Eippert F, Veit R, Anders S (2012) Intentional social distance regulation alters affective responses towards victims of violence: an FMRI study. Hum Brain Mapp 33:2464–2476.
Li F, Yin S, Feng P, Hu N, Ding C, Chen A (2018) The cognitive up- and down-regulation of positive emotion: evidence from behavior, electrophysiology, and neuroimaging. Biol Psychol 136:57–66.
Lindquist KA, Satpute AB, Wager TD, Weber J, Barrett LF (2016) The brain basis of positive and negative affect: evidence from a meta-analysis of the human neuroimaging literature. Cereb Cortex 26:1910–1922.
McRae K, Reiman EM, Fort CL, Chen K, Lane RD (2008) Association between trait emotional awareness and dorsal anterior cingulate activity during emotion is arousal-dependent. Neuroimage 41:648–655.
McRae K, Hughes B, Chopra S, Gabrieli JD, Gross JJ, Ochsner KN (2010) The neural bases of distraction and reappraisal. J Cogn Neurosci 22:248–262.
Morawetz C, Bode S, Baudewig J, Jacobs AM, Heekeren HR (2016a) Neural representation of emotion regulation goals. Hum Brain Mapp 37:600–620.
Morawetz C, Bode S, Baudewig J, Kirilina E, Heekeren HR (2016b) Changes in effective connectivity between dorsal and ventral prefrontal regions moderate emotion regulation. Cereb Cortex 26:1923–1937.
Morawetz C, Alexandrowicz RW, Heekeren HR (2017a) Successful emotion regulation is predicted by amygdala activity and aspects of personality: a latent variable approach. Emotion 17:421–441.
Morawetz C, Bode S, Derntl B, Heekeren HR (2017b) The effect of strategies, goals and stimulus material on the neural mechanisms of emotion regulation: a meta-analysis of fMRI studies. Neurosci Biobehav Rev 72:111–128.
Northoff G, Heinzel A, De Greck M, Bermpohl F, Dobrowolny H, Panksepp J (2006) Self-referential processing in our brain: a meta-analysis of imaging studies on the self. Neuroimage 31:440–457.
Ochsner KN, Gross JJ (2005) The cognitive control of emotion. Trends Cogn Sci 9:242–249.
Ochsner KN, Ray RD, Cooper JC, Robertson ER, Chopra S, Gabrieli JD, Gross JJ (2004) For better or for worse: neural systems supporting the cognitive down-and upregulation of negative emotion. Neuroimage 23:483–499.
Ochsner KN, Silvers JA, Buhle JT (2012) Functional imaging studies of emotion regulation: a synthetic review and evolving model of the cognitive control of emotion. Ann NY Acad Sci 1251:E1–E24.
Okudera T, Huang YP, Fukusumi A, Nakamura Y, Hatazawa J, Uemura K (1999) Micro-angiographical studies of the medullary venous system of the cerebral hemisphere. Neuropathology 19:93–111.
Özbay PS, Chang C, Picchioni D, Mandelkow H, Moehlman TM, Chappel-Farley MG, van Gelderen P, de Zwart JA, Duyn JH (2018) Contribution of systemic vascular effects to fMRI activity in white matter. Neuroimage 176:541–549.
Özbay PS, Chang C, Picchioni D, Mandelkow H, Chappel-Farley MG, van Gelderen P, de Zwart JA, Duyn J (2019) Sympathetic activity contributes to the fMRI signal. Commun Biol 2:1–9.
Phelps EA (2006) Emotion and cognition: insights from studies of the human amygdala. Annu Rev Psychol 57:27–53.
Sokołowski A, Morawetz C, Folkierska-Żukowska M, Dragan W (2021) Brain activation during cognitive reappraisal depending on regulation goals and stimulus valence. Soc Cogn Affect Neurosci nsab117.
Steinfurth EC, Wendt J, Geisler F, Hamm AO, Thayer JF, Koenig J (2018) Resting state vagally-mediated heart rate variability is associated with neural activity during explicit emotion regulation. Front Neurosci 12:794.
Taylor SF, Stern ER, Gehring WJ (2007) Neural systems for error monitoring: recent findings and theoretical perspectives. Neuroscientist 13:160–172.
Woolrich MW, Ripley BD, Brady M, Smith SM (2001) Temporal autocorrelation in univariate linear modeling of FMRI data. Neuroimage 14:1370–1386.
Woolrich MW, Behrens TE, Beckmann CF, Jenkinson M, Smith SM (2004) Multilevel linear modelling for FMRI group analysis using Bayesian inference. Neuroimage 21:1732–1747.